University of Mississippi

eGrove

The spectral features and detectability of small, cyclic silicon carbide clusters

Christopher M. Sehring
Delta State University

C. Zachary Palmer
University of Mississippi

Brent R. Westbrook
University of Mississippi

Ryan C. Fortenberry
University of Mississippi

Recommended Citation

Check for updates

The spectral features and detectability of small, cyclic silicon carbide clusters

Christopher M. Sehring[1], C. Zachary Palmer[2],
Brent R. Westbrook[2] and Ryan C. Fortenberry[2]*

[1]Division of Mathematics and Sciences, Delta State University, Cleveland, MS, United States,
[2]Department of Chemistry and Biochemistry, University of Mississippi, Oxford, MS, United States

Rovibrational spectral data for several tetra-atomic silicon carbide clusters (TASCCs) are computed in this work using a CCSD(T)-F12b/cc-pCVTZ-F12 quartic force field. Accurate theoretical spectroscopic data may facilitate the observation of TASCCs in the interstellar medium which may lead to a more complete understanding of how the smallest silicon carbide (SiC) solids are formed. Such processes are essential for understanding SiC dust grain formation. Due to SiC dust prevalence in the interstellar medium, this may also shed light on subsequent planetary formation. Rhomboidal Si_2C_2 is shown here to have a notably intense (247 km mol^{-1}) anharmonic vibrational frequency at 988.1 cm^{-1} (10.1 μm) for ν_2, falling into one of the spectral emission features typically associated with unknown infrared bands of various astronomical regions. Notable intensities are also present for several of the computed anharmonic vibrational frequencies including the cyclic forms of C_4, SiC_3, Si_3C, and Si_4. These features in the $6-10$ μm range are natural targets for infrared observation with the *James Webb Space Telescope* (JWST)'s MIRI instrument. Additionally, t-Si_2C_2, d-Si_3C, and r-SiC_3 each possess dipole moments of greater than 2.0 D making them interesting targets for radioastronomical searches especially since d-SiC_3 is already known in astrophysical media.

KEYWORDS

vibrational spectroscopy, infrared observations, coupled cluster theory, astrochemistry, carbon chemistry, silicon chemistry

Introduction

Small silicon carbide (SiC) clusters are hypothesized to be an integral step in the process that begins with the nucleosynthesis of carbon and silicon in small, carbonaceous asymptotic giant branch (AGB) stars and leads to the formation of SiC dust grains found in the interstellar medium (ISM) (Mélinon et al., 2007). Several steps along the process of formation from the atomic level to fractal aggregate dust grain structures are not entirely

known (Matthews et al., 2007), but their aggregation is thought to have a direct impact on protoplanetary disk formation. Understanding the composition of stellar atmospheres and nebulae may lead to newfound insight into these processes of dust formation.

The only direct way to study interstellar dust grains is through chemical inspection of primitive chondrite meteorites which accreted before the formation of our Solar System. A chemical isolation technique for SiC dust grains found on primitive chondrite meteorites has long been established (Bernatowicz and Fraundorf., 1987; Nittler and Alexander, 2003) and has shown that SiC dust grains are prevalent in proto-planetary dust clouds. The prevalence of these grains on chondrite meteorites may indicate that SiC species should be targeted for observation in the unidentified infrared/microwave spectra of the interstellar medium.

In addition to terrestrial identification from meteorites containing proto-solar SiC dust grains, some SiC clusters have been accurately identified in stellar environments of carbonaceous AGB stars. The diatomic radical, SiC (Cernicharo and Gottlieb., 1989) along with the triatomic radical (Thaddeus et al., 1984) and closed-shell (Prieto et al., 2015) species of SiC_2 and Si_2C (Cernicharo et al., 2015), have all been identified in the circumstellar envelope of IRC+10216 (CW Leo). The only cyclic tetra-atomic species identified to date in the ISM is SiC_3 (Apponi and McCarthy., 1999a), which was also detected in the aforementioned star IRC+10216. These species have all been detected with rotational spectroscopy. Such observations suggest that the SiC chemistry of these astronomical regions may be richer than has been observed to date. However, the observations so far have been limited to molecules with permanent dipole moments allowing for their detection via rotational spectroscopy. With the new JWST, similar molecules without dipole moments, such as some tetra-atomic silicon carbide clusters (TASCCs), may now be observable by infrared spectroscopy, but the data needed to elucidate such spectra first need to be generated here on Earth.
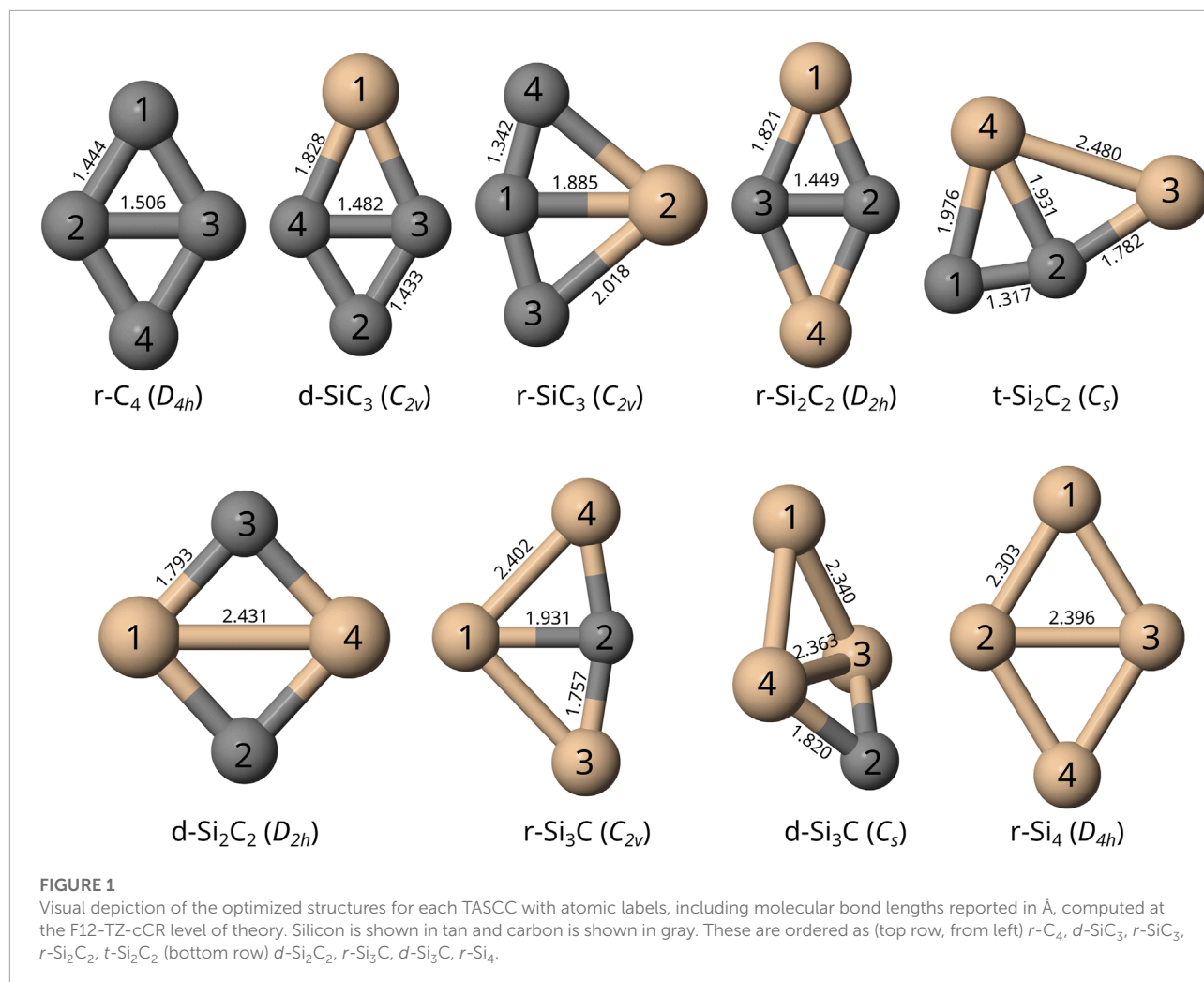
To that end, the spectral data for the pure carbon cluster, rhomboidal (r-)C_4, has been extensively studied both experimentally (Algranati et al., 1989; Blanksby et al., 2000) as well as theoretically (Martin et al., 1996; Martin and Taylor, 1996; Varandas and Rocha, 2018; Wang and Whithey, 2018) at many different levels of theory including at the CCSD(T)/cc-pCV5Z level of theory by Wang and Bowman in 2013 (Wang and Bowman, 2013). In stepping into the silicon analogues of this molecule, cyclic SiC_3 includes two C_{2v} isomers, one exhibiting a transannular C-C bond and the other a transannular Si-C bond. The former will be referred to as diamond SiC_3, or d-SiC_3 hereafter. The d-SiC_3 isomer, in particular has been a focus of previous theoretical and experimental work as it is currently the only cyclic tetra-atomic species identified in the ISM (Apponi and McCarthy., 1999a).

Thus, previous theoretical (Linguerri et al., 2006), experimental microwave spectroscopy (Apponi and McCarthy., 1999b; McCarthy et al., 2019), and astronomically-observed (Apponi and McCarthy., 1999a; McCarthy et al., 2019) spectral data are available. The isomer of SiC_3 with a transannular Si-C bond, which will be referred to as r-SiC_3 hereafter, has been previously studied theoretically (Linguerri et al., 2006) and experimentally (McCarthy et al., 1999). While some spectral data do exist, the complete set of spectral data have yet to be produced especially for vibrational spectra of these SiC_3 isomers. As such, the existing experimental data for these molecules will serve to benchmark the computations performed herein, but new data will also be provided beyond these benchmarks.

Two isomers of Si_2C_2, a rhomboidal D_{2h} structure with a transannular C-C bond and a C_s trapezoidal isomer with a transannular Si-C bond, have been studied experimentally (Presilla-Márquez et al., 1995) using vibrational spectroscopy. The r-Si_2C_2 species with a C-C transannular bond has also been theoretically studied using density functional theory (DFT) at the B3LYP/6-311G(3df) level of theory (Yadav et al., 2006). Trapezoidal (t-)Si_2C_2 and r-Si_2C_2 isomers with transannular Si-Si bonds have only been studied theoretically at the MP2/6-31G* level (Lammertsma and Güner, 1988). A higher level of theory could be useful in corroborating these early computations making more modern computations on these structures necessary.

Two isomers of Si_3C are studied in this work. Like with the SiC_3 isomers, r-Si_3C exhibits a transannular Si-C bond, while d-Si_3C possesses a transannular Si-Si bond. The r-Si_3C isomer has been studied in the laboratory via vibrational spectroscopy (Presilla-Márquez and Graham, 1992; Stanton et al., 2005; Truong et al., 2015). Both isomers have only been theoretically studied in regards to their spectroscopic constants (Rittby, 1992) more than 30 years ago at the Hartree-Fock level of theory. Lastly, only the r-Si_4 cation has been both theoretically and experimentally studied (Savoca et al., 2012). Conversely, theoretical spectral data are currently unavailable for the neutral species of r-Si_4 leaving the door open for a more complete theoretical analysis and spectroscopic characterization of these structures.

Despite all the previous work discussed previously, high level theoretical methods have only been applied to three of the nine TASCCs with various levels of spectral completeness reported. Additionally, one experimental study has investigated the spectral data of heteroatomic TASCCs (Babin et al., 2021), while another study has undertaken DFT analysis with the 6-311G* basis set for various TASCC cations (Lavendy et al., 1997). The current work applies recent advancements in modern approaches to all nine TASCCs herein including the first high-level computations for the remaining six species. By covering every combination of Si and C in a tetra-atomic molecule, this work will examine the effect of silicon doping on the IR emission

FIGURE 1
Visual depiction of the optimized structures for each TASCC with atomic labels, including molecular bond lengths reported in Å, computed at the F12-TZ-cCR level of theory. Silicon is shown in tan and carbon is shown in gray. These are ordered as (top row, from left) r-C_4, d-SiC_3, r-SiC_3, r-Si_2C_2, t-Si_2C_2 (bottom row) d-Si_2C_2, r-Si_3C, d-Si_3C, r-Si_4.

bands for carbide clusters, which previously has only been briefly studied (Inostroza et al., 2008; Savoca et al., 2013), and no work has studied this effect on TASCCs.

In light of a need for modern approaches, this work utilizes quartic force field (QFF) methods to produce highly-accurate, explicit anharmonic vibrational frequencies, rotational constants, and other spectroscopic constants for each of the molecules studied herein. A QFF is a fourth-order Taylor series expansion of the potential portion of the internuclear Watson Hamiltonian (Fortenberry and Lee, 2019). Previous work has shown that QFF techniques produce fundamental anharmonic frequencies that are accurate to within 5–7 cm^{-1} of gas-phase vibrational frequencies and within about 20 MHz of experimental rotational constants (Huang and Lee, 2008, 2009; Huang et al., 2011; Fortenberry et al., 2012; Huang et al., 2013; Fortenberry et al., 2014a, 2015; Zhao et al., 2014; Kitchens and Fortenberry, 2016; Bizzocchi et al., 2017; Fortenberry et al., 2018a; Valiev et al., 2020; Gardner et al., 2021). These constants may be used to aid in

determination of the molecules responsible for unidentified peaks in the infrared and microwave spectra in nebulae, gas clouds, circumstellar envelopes, or other astronomical environments. Accurate characterization of these environments may lead to a more complete understanding of the processes that lead to their evolution possibly including dust nucleation and planet formation. Vibrational observation may be promising for the novel molecules studied herein as *JWST*'s MIRI instrument can resolve spectra at frequencies down to roughly 350 cm^{-1} (28 μm).

Computational methods

The present QFFs are computed at two different levels of theory for each TASCC. Both methods use coupled cluster theory at the singles, doubles, and perturbative triples level (Raghavachari et al., 1989) within the explicitly correlated F12b formalism, or CCSD(T)-F12b (Adler et al., 2007;

TABLE 1 Harmonic (ω) and Fundamental (ν) Vibrational Frequencies (in cm^{-1}) with Intensities (in km mol^{-1}, in Parentheses) for r-C$_4$. Mode descriptions (Desc.) refer to the SICs in Eqns. 1-24.

Mode	Desc	F12-TZ	F12-TZ-cCR	CCSD(T)/cc-pCV5Z[a]
$\omega_1(b_{1u})$	S_5	1388.0	1395.8 (183)	1396.0
$\omega_2(a_g)$	S_1	1265.3	1272.5 (-)	1272.2
$\omega_3(b_{3g})$	S_3	1032.3	1038.1 (-)	1038.9
$\omega_4(a_g)$	S_2	945.0	949.6 (-)	949.6
$\omega_5(b_{2u})$	S_6	538.6	541.1 (26)	539.9
$\omega_6(b_{3u})$	S_4	304.7	306.4 (49)	306.1
$\nu_1(b_{1u})$		1308.0	1315.1 (159)	1314.54
$\nu_2(a_g)$		1245.7	1252.8 (-)	1256.40
$\nu_3(b_{3g})$		997.5	1002.9 (-)	1002.93
$\nu_4(a_g)$		926.6	931.1 (-)	930.11
$\nu_5(b_{2u})$		522.9	525.2 (27)	522.60
$\nu_6(b_{3u})$		304.2	305.9 (47)	302.87

[a]Previous theory, Wang and Bowman (2013).

TABLE 2 Equilibrium ($_e$), vibrationally-averaged ($_0$), and singly-vibrationally excited ($_{n>0}$) principal rotational constants, quartic (Δ/δ) and sextic (Φ/ϕ) distortion constants, principal rotational constants, and quartic for r-C$_4$.

Constant	Units	F12-TZ	F12-TZ-cCR
A_e	MHz	36884.1	37154.2
B_e	MHz	13801.8	13875.6
C_e	MHz	10043.6	10102.7
A_0	MHz	36631.5	36897.8
B_0	MHz	13735.7	13809.2
C_0	MHz	9974.7	10033.3
A_1	MHz	36477.8	36743.3
B_1	MHz	13690.2	13763.4
C_1	MHz	9941.7	10000.0
A_2	MHz	36476.7	36740.7
B_2	MHz	13708.0	13781.6
C_2	MHz	9952.0	10010.5
A_3	MHz	36551.9	36817.4
B_3	MHz	13690.6	13763.9
C_3	MHz	9920.5	9978.8
A_4	MHz	36552.5	36816.1
B_4	MHz	13746.8	13820.6
C_4	MHz	9955.1	10013.5
A_5	MHz	37469.2	37743.9
B_5	MHz	13680.4	13753.9
C_5	MHz	9925.2	9983.5
A_6	MHz	35755.8	36012.8
B_6	MHz	13765.7	13839.3
C_6	MHz	10015.9	10074.7
Δ_J	kHz	6.764	6.803
Δ_K	kHz	160.208	162.249
Δ_{JK}	kHz	21.818	21.935
δ_J	kHz	1.881	1.891
δ_K	kHz	23.617	23.798
Φ_J	mHz	5.603	5.634
Φ_K	Hz	1.325	1.332
Φ_{JK}	mHz	−38.586	−38.920
Φ_{KJ}	mHz	−129.708	−130.439
ϕ_j	mHz	2.694	2.708
ϕ_{jk}	mHz	−6.332	−6.429
ϕ_k	Hz	1.208	1.225

Peterson et al., 2008; Knizia et al., 2009; Huang et al., 2010). The first QFF method utilizes the cc-pVTZ-F12 basis set alone, and this combination will henceforth be abbreviated as "F12-TZ". F12-TZ has been shown to yield accurate results for vibrational frequencies, within 5–7 cm^{-1} compared to gas-phase experiment, and it still exhibits far greater time savings than previously used composite, coupled cluster methods (Agbaglo et al., 2019; Agbaglo and Fortenberry, 2019a,b; Gardner et al., 2021). The second QFF method employs the cc-pCVTZ-F12 (Hill and Peterson, 2010) basis set to include the effects from core electron correlation (cC) with additional corrections for scalar relativity (R). This composite method is hereafter abbreviated "F12-TZ-cCR" (Watrous et al., 2021). In addition to including core correlation in the computation, the F12-TZ-cCR method utilizes Douglas-Kroll scalar relativistic corrections (Douglas and Kroll, 1974) in its single-point energy computations at the CCSD(T)/cc-pVTZ-DK level of theory to produce a more accurate description of the potential energy surface for an increased computational cost relative to F12-TZ that is still far less than the composite methods used previously.

All of the QFFs reported in this work are computed in the same, general manner beginning with the optimization of the molecular geometry with the CCSD(T)-F12b method whether excluding (F12-TZ) or including (F12-TZ-cCR) core electron correlation in the computation. All also utilize the MOLPRO 2020.1 quantum chemical program (Werner et al., 2020). The resulting optimized geometry serves as a reference point from which the INTDER program (Allen., 2005) displaces bond lengths and angles/torsions by 0.005 Å and radians, respectively (Huang and Lee, 2008). For the tetra-atomic D$_{4h}$ and D$_{2h}$ molecules, such as rhomboidal C$_4$ and Si$_4$ and the rhomboidal and diamond isomers of Si$_2$C$_2$, 233 displacement points are required utilizing the following symmetry-internal coordinates

TABLE 3 Equilibrium ($_e$), vibrationally-averaged ($_0$), and singly-vibrationally excited ($_{n>0}$) principal rotational constants, quartic (Δ/δ) and sextic (Φ/ϕ) distortion constants, and dipole moments (μ) for SiC$_3$ Isomers.

Constant	Units	d-SiC$_3$			r-SiC$_3$		
		F12-TZ	F12-TZ-cCR	Previous Expt.[a]	F12-TZ	F12-TZ-cCR	Previous Expt.[b]
A_e	MHz	38038.3	38353.3		12410.8	12491.2	
B_e	MHz	6266.0	6305.8		11332.8	11419.4	
C_e	MHz	5379.8	5415.5		5923.6	5965.6	
A_0	MHz	37713.4	38026.4	37950.7	12403.5	12483.9	12474.3
B_0	MHz	6241.1	6280.7	6283.0	11257.0	11342.5	11345.1
C_0	MHz	5350.3	5385.8	5386.8	5895.9	5937.5	5936.2
A_1	MHz	37585.8	37898.1		12323.2	12403.4	
B_1	MHz	6225.7	6265.3		11298.1	11383.6	
C_1	MHz	5336.8	5372.2		5890.7	5932.2	
A_2	MHz	37686.6	38000.8		12356.5	12436.6	
B_2	MHz	6220.8	6260.3		11263.5	11349.0	
C_2	MHz	5332.5	5367.8		5886.1	5927.6	
A_3	MHz	37324.6	37632.5		12423.9	12504.6	
B_3	MHz	6242.8	6282.7		11214.4	11299.5	
C_3	MHz	5339.6	5375.1		5881.8	5923.3	
A_4	MHz	37678.0	37992.3		12385.6	12465.9	
B_4	MHz	6230.3	6269.7		11242.0	11327.2	
C_4	MHz	5336.8	5372.1		5875.4	5916.8	
A_5	MHz	37722.9	38035.6		12413.2	12493.7	
B_5	MHz	6223.4	6263.1		11198.5	11283.3	
C_5	MHz	5328.8	5364.2		5856.5	5897.6	
A_6	MHz	37632.2	37945.3		12504.0	12584.9	
B_6	MHz	6253.7	6293.2		11173.7	11258.6	
C_6	MHz	5368.6	5404.1		5929.0	5970.8	
Δ_J	kHz	1.617	1.634		9.085	9.216	
Δ_K	kHz	237.495	238.762		0.000	0.000	
Δ_{JK}	kHz	8.120	8.161		20.559	20.860	
δ_J	Hz	260.571	262.815		3684	3738	
δ_K	kHz	10.218	10.308		19.036	19.310	
Φ_J	μHz	228.827	228.657		7861	8013	
Φ_K	mHz	949.770	935.446		-106.231	-109.143	
Φ_{JK}	mHz	-14.085	-13.928		-181.217	-186.481	
Φ_{KJ}	mHz	-237.178	-237.086		287.878	296.036	
ϕ_j	μHz	138.857	139.332		4107	4188	
ϕ_{jk}	mHz	-5.426	-5.404		-90.403	-93.051	
ϕ_k	mHz	984.051	992.679		179.137	182.597	
μ	D	4.03			2.07		

[a]McCarthy et al. (2019).
[b]McCarthy et al. (1999).

(SICs) with atomic labels, as shown in **Figure 1**. QFFs of this connectivity have previously employed such a coordinate system (Westbrook and Fortenberry, 2020).

$$S_1\left(a_g\right) = \frac{1}{\sqrt{2}}\left[r(\mathrm{Si}_1 - \mathrm{Si}_4) + r(\mathrm{C}_2 - \mathrm{C}_3)\right] \tag{1}$$

$$S_2\left(a_g\right) = \frac{1}{\sqrt{2}}\left[r(\mathrm{Si}_1 - \mathrm{Si}_4) - r(\mathrm{C}_2 - \mathrm{C}_3)\right] \tag{2}$$

$$S_3\left(b_{3g}\right) = \frac{1}{2}\left[r(\mathrm{Si}_1 - \mathrm{C}_2) - r(\mathrm{Si}_1 - \mathrm{C}_3) - r(\mathrm{C}_2 - \mathrm{Si}_4) + r(\mathrm{C}_3 - \mathrm{Si}_4)\right] \tag{3}$$

$$S_4\left(b_{3u}\right) = \tau\left(\mathrm{Si}_4 - \mathrm{C}_3 - \mathrm{C}_2 - \mathrm{Si}_1\right) \tag{4}$$

$$S_5\left(b_{1u}\right) = \frac{1}{2}\left[r(\mathrm{Si}_1 - \mathrm{C}_2) + r(\mathrm{Si}_1 - \mathrm{C}_3) - r(\mathrm{C}_2 - \mathrm{Si}_4) - r(\mathrm{C}_3 - \mathrm{Si}_4)\right] \tag{5}$$

$$S_6\left(b_{2u}\right) = \frac{1}{2}\left[r(\mathrm{Si}_1 - \mathrm{C}_2) - r(\mathrm{Si}_1 - \mathrm{C}_3) + r(\mathrm{C}_2 - \mathrm{Si}_4) - r(\mathrm{C}_3 - \mathrm{Si}_4)\right] \tag{6}$$

Differently, 413 displacement points, as employed previously (Fortenberry et al., 2013; Bassett and Fortenberry, 2018), are computed for the cyclic C$_{2v}$ molecules (r-Si$_3$C and d-SiC$_3$)

TABLE 4 Harmonic (ω) and Fundamental (ν) Vibrational Frequencies (in cm^{-1}) with Intensities (in km mol^{-1}, in Parentheses) and Relative Energies (in kcal mol^{-1}) for SiC$_3$ Isomers. Mode descriptions (Desc.) refer to the SICs in Eqns. 1-24.

Isomer	Rel. E	Mode	Desc	F12-TZ	F12-TZ-cCR	CCSD(T)/cc-pVQZ[a]
d-SiC$_3$	0.0	$\omega_1(a_1)$	$1.109\,S_2 + 0.079 S_1$	1394.5	1402.3 (166)	1390
		$\omega_2(b_2)$	$0.950 S_4 - 0.050 S_5$	1052.2	1057.6 (5)	1048
		$\omega_3(a_1)$	S_3	992.4	1001.2 (29)	985
		$\omega_4(a_1)$	$1.073\,S_1 + 0.099 S_2$	692.1	695.6 (41)	688
		$\omega_5(b_2)$	$0.950\,S_5 + 0.050 S_4$	431.9	435.5 (35)	427
		$\omega_6(b_1)$	S_6	248.0	250.0 (9)	246
		$\nu_1(a_1)$		1332.4	1339.4 (128)	1348
		$\nu_2(b_2)$		1022.2	1027.2 (4)	1026
		$\nu_3(a_1)$		971.1	980.0 (23)	968
		$\nu_4(a_1)$		677.8	680.9 (38)	671
		$\nu_5(b_2)$		423.2	426.3 (34)	410
		$\nu_6(b_1)$		248.6	249.9 (8)	243
r-SiC$_3$	6.1	$\omega_1(b_2)$	$0.924 S_5 + 0.076 S_4$	1556.8	1566.3 (79)	1555
		$\omega_2(a_1)$	$0.586 S_3 + 0.252 S_2 + 0.162 S_1$	1132.6	1140.4 (-)	1129
		$\omega_3(a_1)$	$0.876 S_1 - 0.126 S_3$	805.6	809.1 (55)	804
		$\omega_4(a_1)$	$0.750 S_2 - 0.288 S_3$	523.0	525.5 (10)	519
		$\omega_5(b_2)$	$0.924 S_4 - 0.076 S_5$	420.6	421.9 (2)	416
		$\omega_6(b_1)$	S_6	169.2	170.7 (54)	173
		$\nu_1(b_2)$		1516.3	1525.5 (77)	1527
		$\nu_2(a_1)$		1118.8	1126.5 (-)	1107
		$\nu_3(a_1)$		790.5	793.8 (54)	821
		$\nu_4(a_1)$		511.8	514.2 (9)	495
		$\nu_5(b_2)$		411.1	412.2 (2)	398
		$\nu_6(b_1)$		190.2	191.2 (50)	188

[a]Previous theory, Linguerri et al. (2006).

incorporating the following SICs with atom labels given in **Figure 1**.

$$S_1(a_1) = r(\text{Si}_1 - \text{C}_2) \tag{7}$$

$$S_2(a_1) = \frac{1}{\sqrt{2}}\left[r(\text{C}_2 - \text{C}_3) + r(\text{C}_2 - \text{C}_4)\right] \tag{8}$$

$$S_3(a_1) = \frac{1}{\sqrt{2}}\left[\angle(\text{Si}_1 - \text{C}_2 - \text{C}_3) + \angle(\text{Si}_1 - \text{C}_2 - \text{C}_4)\right] \tag{9}$$

$$S_4(b_2) = \frac{1}{\sqrt{2}}\left[r(\text{C}_2 - \text{C}_3) - r(\text{C}_2 - \text{C}_4)\right] \tag{10}$$

$$S_5(b_2) = \frac{1}{\sqrt{2}}\left[\angle(\text{Si}_1 - \text{C}_2 - \text{C}_3) - \angle(\text{Si}_1 - \text{C}_2 - \text{C}_4)\right] \tag{11}$$

$$S_6(b_1) = \tau(\text{Si}_1 - \text{C}_2 - \text{C}_3 - \text{C}_4) \tag{12}$$

Furthermore, 665 points are used for the C$_s$ molecule in this study (d-Si$_3$C) with the following SICs from earlier work (Fortenberry et al., 2018b, 2019; Fortenberry, 2019) with atomic labels, shown in **Figure 1**.

$$S_1(a_1) = r(\text{Si}_1 - \text{C}_2) \tag{13}$$

$$S_2(a_1) = \frac{1}{\sqrt{2}}\left[r(\text{C}_2 - \text{Si}_3) + r(\text{C}_2 - \text{Si}_4)\right] \tag{14}$$

$$S_3(b_2) = \frac{1}{\sqrt{2}}\left[\angle(\text{Si}_1 - \text{C}_2 - \text{Si}_3) + \angle(\text{Si}_1 - \text{C}_2 - \text{Si}_4)\right] \tag{15}$$

$$S_4(b_2) = \angle(\text{Si}_3 - \text{C}_2 - \text{Si}_4) \tag{16}$$

$$S_5(a_1) = \frac{1}{\sqrt{2}}\left[r(\text{C}_2 - \text{Si}_3) - r(\text{C}_2 - \text{Si}_4)\right] \tag{17}$$

$$S_6(b_1) = \frac{1}{\sqrt{2}}\left[\angle(\text{Si}_1 - \text{C}_2 - \text{Si}_3) - \angle(\text{Si}_1 - \text{C}_2 - \text{Si}_4)\right] \tag{18}$$

Finally, 743 symmetry-unique (for a total of 805) points, as incorporated in previous work (Fortenberry et al., 2011, 2012, 2020), are used for the planar C$_s$ molecule in this study (t-Si$_2$C$_2$). The SICs for such a connectivity are labeled as shown in **Figure 1**.

$$S_1(a') = r(\text{C}_1 - \text{C}_2) \tag{19}$$

$$S_2(a') = r(\text{C}_2 - \text{Si}_3) \tag{20}$$

$$S_3(a') = r(\text{Si}_3 - \text{Si}_4) \tag{21}$$

TABLE 5 Harmonic (ω) and Fundamental (v) Vibrational Frequencies (in cm^{-1}) with Intensities (in km mol^{-1}, in Parentheses) and Relative Energies (in kcal mol^{-1}) for Si$_2$C$_2$ Isomers. Mode descriptions (Desc.) refer to the SICs in Eqns. 1-24.

Isomer	Rel. E	Mode	Desc	F12-TZ	F12-TZ-cCR	Previous Expt.[a]
r-Si$_2$C$_2$[b]	0.0	$\omega_1(a_g)$	$0.719S_1 - 0.281S_2$	1078.7	1089.3 (-)	
		$\omega_2(b_{1u})$	S_5	1003.1	1006.7 (263)	
		$\omega_3(b_{3g})$	S_3	981.0	984.9 (-)	
		$\omega_4(a_g)$	$0.719 S_2 + 0.281S_1$	522.8	525.5 (-)	
		$\omega_5(b_{2u})$	S_6	386.0	388.5 (57)	
		$\omega_6(b_{3u})$	S_4	199.4	200.4 (3)	
		$v_1(a_g)$		1060.3	1069.7 (-)	
		$v_2(b_{1u})$		984.3	988.1 (247)	982.9
		$v_3(b_{3g})$		960.9	964.7 (-)	
		$v_4(a_g)$		517.5	520.1 (-)	
		$v_5(b_{2u})$		380.6	383.0 (56)	382.2
		$v_6(b_{3u})$		199.1	199.2 (3)	
d-Si$_2$C$_2$	83.8	$\omega_1(a_g)$	$0.916 S_1 - 0.084S_2$	852.2	857.5	
		$\omega_2(b_{2u})$	S_5	739.7	744.0	
		$\omega_3(b_{1u})$	S_4	705.4	707.5	
		$\omega_4(b_{3g})$	S_3	486.7	491.5	
		$\omega_5(a_g)$	$0.916 S_2 + 0.084S_1$	478.3	480.2	
		$v_1(a_g)$		824.9	830.7	
		$v_2(b_{2u})$		716.3	720.5	
		$v_3(b_{1u})$		686.6	688.9	
		$v_4(b_{3g})$		479.6	484.3	
		$v_5(a_g)$		462.0	464.7	
t-Si$_2$C$_2$	7.5	$\omega_1(a')$	$0.906S_1 - 0.074S_2$	1549.7	1558.2 (24)	
		$\omega_2(a')$	$0.400 S_5 - 0.310S_4 - 0.231S_2 - 0.056S_1$	727.2	730.9 (27)	
		$\omega_3(a')$	$0.712 S_2 + 0.231S_5 + 0.129S_3 - 0.102S_4$	643.9	647.5 (66)	
		$\omega_4(a')$	$0.839 S_4 + 0.188S_5$	516.0	518.6 (4)	
		$\omega_5(a')$	$0.864 S_3 - 0.158S_5 + 0.044S_4$	309.6	309.6 (1)	
		$\omega_6(a'')$	S_6	195.9	196.1 (14)	
		$v_1(a')$		1528.1	1537.6 (23)	1538.0
		$v_2(a')$		719.8	724.1 (26)	
		$v_3(a')$		635.2	636.9 (63)	632.0
		$v_4(a')$		506.8	509.1 (3)	
		$v_5(a')$		306.5	301.0 (1)	
		$v_6(a'')$		215.4	173.5 (13)	

[a]Presilla-Márquez et al. (1995).
[b]Isomer with the transannular C-C bond.

$$S_4(a') = \angle(C_1 - C_2 - Si_3) \quad (22)$$

$$S_5(a') = \angle(C_2 - Si_3 - Si_4) \quad (23)$$

$$S_6(a'') = \tau(Si_4 - Si_3 - C_2 - C_1) \quad (24)$$

Regardless of the number of displacements, single-point energy computations are conducted at both levels of theory for each of the molecules analyzed in this work. Once the single-point energy computations finish, their relative energies are fit to a potential function by a least squares procedure with sums of squared residual values of better than 10^{-16} a. u.^{2}, excluding d-Si$_3$C, r-SiC$_3$, and t-Si$_2$C$_2$/d-SiC$_3$ which have slightly higher

residuals of 10^{-13}, 10^{-14}, and 10^{-15} a. u.^{2}, respectively. The QFF is then refit including corrections from the initial fitting to produce the final equilibrium geometry and zero-gradient force constants. The INTDER program (Allen., 2005) then converts the force constants from SICs into Cartesian coordinates. The Cartesian force constants provide greater flexibility for use in the SPECTRO program (Gaw et al., 1991), which utilizes second-order rotational and vibrational perturbation theory (Mills, 1972; Watson, 1977; Papousek and Aliev, 1982) (VPT2) to produce highly-accurate rovibrational constants and fundamental vibrational frequencies. SPECTRO also incorporates Fermi resonances as well as resonance polyads (Martin and Taylor, 1997), of the **Supplementary Material**, to

TABLE 6 Equilibrium ($_e$), vibrationally-averaged ($_0$), and singly-vibrationally excited ($_{n>0}$) principal rotational constants, quartic (Δ/δ) and sextic (Φ/ϕ) distortion constants, and dipole moments (μ) for Si_2C_2 Isomers.

Constant	Units	r-Si_2C_2		d-Si_2C_2		t-Si_2C_2	
		F12-TZ	F12-TZ-cCR	F12-TZ	F12-TZ-cCR	F12-TZ	F12-TZ-cCR
A_e	MHz	39831.0	40141.9	12029.5	12131.1	11579.8	11688.3
B_e	MHz	3210.8	3233.0	6067.5	6113.1	4830.3	4864.7
C_e	MHz	2971.2	2991.9	4033.1	4064.9	3408.3	3435.0
A_0	MHz	39517.1	39826.7	11988.8	12090.0	11513.2	11620.5
B_0	MHz	3199.6	3221.8	6014.8	6060.5	4821.9	4856.5
C_0	MHz	2958.9	2979.6	4000.0	4031.5	3395.1	3421.6
A_1	MHz	38901.6	39208.6	11972.4	12073.7	11543.8	11651.6
B_1	MHz	3208.4	3230.7	6000.0	6045.5	4804.7	4839.2
C_1	MHz	2961.7	2982.4	3992.2	4023.7	3389.5	3415.9
A_2	MHz	39529.4	39839.3	11999.5	12100.9	11494.1	11601.1
B_2	MHz	3185.3	3207.3	5992.9	6038.5	4809.5	4843.9
C_2	MHz	2946.9	2967.5	3986.2	4017.6	3385.7	3412.1
A_3	MHz	39537.7	39848.8	11925.7	12026.6	11469.3	11575.9
B_3	MHz	3187.8	3209.9	6025.3	6071.1	4829.1	4863.8
C_3	MHz	2947.7	2968.2	3991.9	4023.3	3392.2	3418.6
A_4	MHz	39509.8	39819.8	12000.5	12101.4	11427.3	11533.0
B_4	MHz	3194.9	3217.0	5960.2	6006.0	4837.7	4872.6
C_4	MHz	2953.4	2974.0	3968.9	4000.4	3392.7	3419.2
A_5	MHz	39506.2	39815.4	12018.1	12118.8	11559.2	11666.9
B_5	MHz	3194.1	3216.3	6010.4	6056.7	4797.3	4831.9
C_5	MHz	2951.7	2972.4	3996.2	4027.9	3376.3	3402.7
A_6	MHz	39489.9	39798.1	11935.5	12036.0	11452.6	11559.2
B_6	MHz	3205.0	3227.3	5994.3	6039.7	4836.5	4871.4
C_6	MHz	2967.0	2987.8	3998.2	4029.7	3407.3	3434.0
Δ_J	Hz	439.138	444.353	2219	2253	1818	1854
Δ_K	kHz	277.086	277.585	9.730	9.980	16.086	16.314
Δ_{JK}	kHz	0.000	0.000	2.827	2.737	3.401	3.520
δ_J	Hz	41.274	41.649	800.777	812.913	566.558	576.924
δ_K	kHz	2.614	2.647	6.061	6.096	5.497	5.635
Φ_J	μHz	22.113	22.846	2024	2124	−1671	−1713
Φ_K	mH	−173.310	−168.405	10.910	13.678	−9.679	−9.929
Φ_{JK}	mHz	−1.577	−1.611	−65.246	−64.794	12.606	13.392
Φ_{KJ}	mHz	42.002	42.591	104.525	102.066	−1.250	−1.012
ϕ_j	μHz	12.940	13.136	1001	1049	−715.437	−733.169
ϕ_{jk}	μHz	−372.535	−375.455	−30316	−29836	−6716	−6739
ϕ_k	mHz	317.768	320.509	83.273	84.465	128.887	133.943
μ	D	-		-		2.90	

increase the accuracy of the computed fundamental anharmonic vibrational frequencies and rotational constants. Coriolis resonances are included in the rotational constant computations, as well.

Additionally, the Gaussian16 (Frisch et al., 2016) program is used to compute transition intensities for each anharmonic vibrational frequency at the MP2/cc-pVDZ level of theory. This method has been shown to produce semi-quantitative accuracy for anharmonic infrared intensities at a low computational cost (Fortenberry et al., 2014b). Finally, dipole moments for each molecule are computed using the Molpro 2020.1 quantum chemical program (Werner et al., 2020).

Results and discussion

The fundamental anharmonic frequencies for r-C_4 from a CCSD(T)/cc-pCV5Z semi-global potential energy surface within a variational approach (Wang and Bowman, 2013) compare well with the QFF VPT2 current data provided in **Table 1**. In each of these tables, ω represents the harmonic values of the vibrational frequencies, v represents the anharmonic values, and the description of the modes (Desc.) is given in terms of the SICs from the previous section. These values all fall within 3.6 cm^{-1} (v_2) and 1.00% (v_6) of the F12-TZ-cCR data in this work while averaging a 1.8 cm^{-1} (0.32%) difference. Such correlation suggests that the F12-TZ-cCR QFF

TABLE 7 Harmonic (ω) and Fundamental (ν) Vibrational Frequencies (in cm^{-1}) with Intensities (in km mol^{-1}, in Parentheses) and Relative Energies (in kcal mol^{-1}) for Si$_3$C Isomers. Mode descriptions (Desc.) refer to the SICs in Eqns. 1-24.

Isomer	Rel. E	Mode	Desc	F12-TZ	F12-TZ-cCR	Previous Expt.[a]
d-Si$_3$C	49.6	$\omega_1(a_1)$	$1.067S_2 - 0.081S_3$	747.1	753.1 (2)	
		$\omega_2(b_2)$	S_5	687.2	692.1 (8)	
		$\omega_3(a_1)$	$0.537S_4 + 0.422S_3 + 0.073S_1$	462.9	464.0 (1)	
		$\omega_4(a_1)$	$0.719\,S_1 - 0.685S_4 - 0.382S_3$	401.0	402.6 (15)	
		$\omega_5(b_2)$	S_6	282.7	282.8 (1)	
		$\omega_6(b_1)$	$1.041\,S_3 + 0.202S_4 - 0.174S_1$	155.7	156.7 (63)	
		$\nu_1(a_1)$		737.9	742.7 (2)	
		$\nu_2(b_2)$		669.4	672.0 (7)	
		$\nu_3(a_1)$		456.7	457.5 (1)	
		$\nu_4(a_1)$		397.4	398.5 (14)	
		$\nu_5(b_2)$		278.4	277.9 (1)	
		$\nu_6(b_1)$		144.6	144.9 (60)	
r-Si$_3$C	0.0	$\omega_1(b_2)$	S_4	1113.8	1118.4 (84)	
		$\omega_2(a_1)$	$0.842\,S_1 + 0.220S_2 - 0.062S_3$	663.7	668.9 (40)	
		$\omega_3(a_1)$	$0.751\,S_2 + 0.133S_3 - 0.116S_1$	512.8	515.4 (17)	
		$\omega_4(a_1)$	S_5	368.4	369.0 (9)	
		$\omega_5(b_2)$	$0.929\,S_3 + 0.043S_1$	314.8	315.4 (4)	
		$\omega_6(b_1)$	S_6	170.5	172.1 (-)	
		$\nu_1(b_2)$		1095.9	1100.3 (80)	1101.4
		$\nu_2(a_1)$		656.5	661.4 (39)	658.2
		$\nu_3(a_1)$		505.2	506.4 (17)	511.8
		$\nu_4(a_1)$		362.3	363.4 (9)	357.6
		$\nu_5(b_2)$		308.6	307.0 (4)	309.5
		$\nu_6(b_1)$		174.4	165.5 (-)	

[a] Presilla-Márquez and Graham (1992).

VPT2 treatment is handling the system well. In contrast, the F12-TZ values do not compare as well as the F12-TZ-cCR data to the previously determined CCSD(T)/cc-pCV5Z data. The ν_2 frequency has the largest absolute difference of 10.7 cm^{-1} (0.85%), and the difference for the total set averages 4.6 cm^{-1} (0.46%). Thus, the F12-TZ-cCR method may come at the optimal ratio of accuracy and computational efficiency for chemical systems of the current nature. Equilibrium ($_e$), vibrationally-averaged ($_0$), and singly-vibrationally excited ($_{n>0}$) rotational constants for r-C$_4$ can be found in Table 2, along with the quartic (Δ and δ) and sextic (Φ and ϕ) distortion coefficients in the Watson A-reduced Hamiltonian and the dipole moment (μ), which by symmetry is zero in this case. The vibrational frequency at 1315.1 cm^{-1} (ν_1) is the best candidate for potential vibrational observation as the frequency is above the ~350 cm^{-1} cutoff for *JWST*'s MIRI, and the intensity is notable with a value of 159 km mol^{-1}. The antisymmetric stretch of water, used here as a familiar basis for comparison, has an intensity of 70 km mol^{-1} implying that this frequency in r-C$_4$ has a higher oscillator strength by more than a factor of two.

The d-SiC$_3$ structure is found to be the lowest energy cyclic isomer for the first silicon replacement analogue. It lies approximately 6.1 kcal mol^{-1} below r-SiC$_3$. The d-SiC$_3$ F12-TZ-cCR rotational constants compare well with

previously determined experimental values by McCarthy et al. (McCarthy et al., 2019). The experimental and present theoretical F12-TZ-cCR spectroscopic constants found in Table 3 differ by just 0.20% for A_0, 0.04% for B_0, and 0.02% for C_0, suggesting high-accuracy for the current method. The dipole moment of d-SiC$_3$ is computed to be 4.03 D, comparing well with previous work (Alberts et al., 1990) which determined the dipole moment to be 4.2 D. This large dipole moment is likely the cause of d-SiC$_3$'s previous detection in the ISM. F12-TZ-cCR rotational constants for r-SiC$_3$ compare well with experimental values determined by McCarthy et al. (McCarthy et al., 1999), with the A_0, B_0, and C_0 constants displaying differences of 0.08%, 0.02%, and 0.02%, respectively. The r-SiC$_3$ isomer is shown to have a dipole moment of 2.07 D, also comparing well with a previous 2.2 D value (Alberts et al., 1990). The strength of the dipole moment for r-SiC$_3$ may also lead to its radioastronomical detection. However, the slightly higher relative energy of this isomer and roughly half dipolar strength of the d isomer imply that the r isomer will likely have a notably smaller emission profile.

Differently, all harmonic frequencies reported for d-SiC$_3$ and r-SiC$_3$, found in Table 4, at the F12-TZ-cCR level provided herein exhibit notable deviations from previous theoretical work done by Linguerri et al. (2006) at the CCSD(T)/cc-pVQZ

TABLE 8 Equilibrium ($_e$), vibrationally-averaged ($_0$), and singly-vibrationally excited ($_{n>0}$) principal rotational constants, quartic (Δ/δ) and sextic (Φ/ϕ) distortion constants, and dipole moments (μ) for Si_3C Isomers.

Constant	Units	d-Si_3C		r-Si_3C	
		F12-TZ	F12-TZ-cCR	F12-TZ	F12-TZ-cCR
A_e	MHz	6229.7	6283.9	8548.3	8626.5
B_e	MHz	4215.7	4255.6	2975.7	2997.9
C_e	MHz	2574.6	2598.3	2207.4	2224.8
A_0	MHz	6228.7	6282.9	8498.3	8574.4
B_0	MHz	4190.0	4229.3	2970.2	2992.5
C_0	MHz	2557.8	2581.4	2199.2	2216.6
A_1	MHz	6220.0	6274.0	8547.2	8623.6
B_1	MHz	4185.9	4225.1	2950.5	2972.6
C_1	MHz	2552.5	2576.0	2192.0	2209.3
A_2	MHz	6232.7	6286.9	8450.3	8525.2
B_2	MHz	4178.9	4218.1	2972.0	2994.4
C_2	MHz	2555.1	2578.6	2195.6	2212.9
A_3	MHz	6209.5	6263.5	8504.6	8580.9
B_3	MHz	4185.6	4224.8	2967.2	2989.4
C_3	MHz	2550.2	2573.7	2196.8	2214.1
A_4	MHz	6213.6	6267.9	8440.5	8515.8
B_4	MHz	4193.7	4232.8	2970.6	2992.9
C_4	MHz	2554.8	2578.3	2192.7	2209.9
A_5	MHz	6230.7	6284.9	8488.6	8564.6
B_5	MHz	4175.0	4214.0	2969.0	2991.4
C_5	MHz	2550.0	2573.4	2196.3	2213.6
A_6	MHz	6263.6	6317.9	8458.6	8531.9
B_6	MHz	4169.2	4208.4	2981.0	3003.4
C_6	MHz	2551.0	2574.5	2206.0	2223.2
Δ_J	Hz	1453	1485	305.354	310.115
Δ_K	kHz	5.439	5.538	13.425	13.728
Δ_{JK}	kHz	0.000	0.000	3.726	3.825
δ_J	Hz	496.534	507.600	58.969	59.474
δ_K	kHz	2.010	2.054	1.818	1.857
Φ_J	μHz	970.090	1001	16.430	17.281
Φ_K	mHz	24.473	24.819	92.259	95.198
Φ_{JK}	mHz	−10.177	−10.646	2.988	3.082
Φ_{KJ}	μHz	823.430	1252	−41670	−42841
ϕ_j	μHz	442.034	456.609	6.322	6.565
ϕ_{jk}	mHz	−4.522	−4.732	1.512	1.562
ϕ_k	mHz	22.870	23.636	23.430	24.322
μ	D	2.64		0.07	

level of theory. The largest differences are 16.2 cm^{-1} (ω_3 from d-SiC_3; 1.64%) and 11.4 cm^{-1} (ω_2 from r-SiC_3; 1.01%). Linguerri et al. (2006) also report fundamental anharmonic frequencies using VSCF for both cyclic isomers of SiC_3. These values compare poorly for both isomers with fundamental frequencies differing by up to 16.3 cm^{-1} (ν_5; 3.98%) and 27.2 cm^{-1} (ν_3; 3.31%) for the presently analyzed d-SiC_3 and r-SiC_3 isomers' F12-TZ-cCR data, respectively. Such poor comparison of the anharmonic frequencies is to be expected for the relatively poor agreement in the harmonic frequencies. The most obvious difference between the present and previous studies is the inclusion of core electron correlation (or lack thereof). As a result, the present F12-TZ-cCR results should be producing more accurate data for subsequent experimental or observational comparison. Additionally, potentially observable fundamental

frequencies for r-SiC_3 include ν_1 at 1525.5 cm^{-1} and ν_3 at 793.8 cm^{-1} with intensities of 77 and 54 km mol^{-1}, respectively, given favorable ISM conditions.

With the accuracy of the current methods benchmarked on the aforementioned species, this work presents the first high level theoretical data for the remaining isomers herein. Relative energies computed at the F12-TZ-cCR level for the three cyclic Si_2C_2 isomers determine that r-Si_2C_2 with the transannular C-C bond is the lowest energy isomer, followed by t-Si_2C_2, which is 7.5 kcal mol^{-1} higher in energy, and, lastly, the other d-Si_2C_2 isomer with the transannular Si-Si bond resides 83.8 kcal mol^{-1} higher in energy. Experimental matrix studies are available for ν_2, shown to be 988.1 cm^{-1} in this work, and ν_5, 383.0 cm^{-1} here, for r-Si_2C_2 with a transannular C-C bond (Presilla-Márquez et al., 1995). These

TABLE 9 Harmonic (ω) and Fundamental (ν) Vibrational Frequencies (in cm^{-1}) with Intensities (in km mol^{-1}, in Parentheses) for r-Si$_4$. Mode descriptions (Desc.) refer to the SICs in Eqns. 1-24.

Mode	Desc	F12-TZ	F12-TZ-cCR
$\omega_1(b_{1u})$	S_5	511.2	512.5 (43)
$\omega_2(a_g)$	S_1	477.8	479.2 (-)
$\omega_3(b_{3g})$	S_3	440.1	442.4 (-)
$\omega_4(a_g)$	S_2	351.2	353.0 (-)
$\omega_5(b_{2u})$	S_6	254.5	254.0 (1)
$\omega_6(b_{3u})$	S_4	75.7	75.1 (4)
$\nu_1(b_{1u})$		504.1	505.9 (41)
$\nu_2(a_g)$		474.1	476.1 (-)
$\nu_3(b_{3g})$		433.8	436.6 (-)
$\nu_4(a_g)$		348.2	350.0 (-)
$\nu_5(b_{2u})$		251.8	251.9 (1)
$\nu_6(b_{3u})$		76.5	76.2 (4)

TABLE 10 Equilibrium ($_e$), vibrationally-averaged ($_0$), and singly-vibrationally excited ($_{n>0}$) principal rotational constants, quartic (Δ/δ) and sextic (Φ/ϕ) distortion constants, principal rotational constants, and quartic for r-Si$_4$.

Constant	Units	F12-TZ	F12-TZ-cCR
A_e	MHz	6232.4	6294.7
B_e	MHz	2312.9	2334.5
C_e	MHz	1686.9	1702.8
A_0	MHz	6207.2	6269.0
B_0	MHz	2308.3	2329.6
C_0	MHz	1682.3	1698.3
A_1	MHz	6197.6	6259.3
B_1	MHz	2303.9	2325.2
C_1	MHz	1679.8	1695.7
A_2	MHz	6191.3	6252.9
B_2	MHz	2306.3	2327.6
C_2	MHz	1680.0	1695.8
A_3	MHz	6204.7	6266.4
B_3	MHz	2303.5	2324.8
C_3	MHz	1678.3	1694.2
A_4	MHz	6195.4	6257.1
B_4	MHz	2310.1	2331.4
C_4	MHz	1681.0	1696.9
A_5	MHz	6205.1	6266.8
B_5	MHz	2302.8	2324.1
C_5	MHz	1678.0	1693.9
A_6	MHz	6198.6	6259.9
B_6	MHz	2313.5	2335.2
C_6	MHz	1687.7	1703.9
Δ_J	Hz	240.115	245.112
Δ_K	kHz	5.528	5.639
Δ_{JK}	Hz	354.517	360.887
δ_J	Hz	67.441	68.721
δ_K	Hz	656.879	667.908
Φ_J	μHz	47.884	49.236
Φ_K	mHz	3.688	3.845
Φ_{JK}	μHz	−593.904	−611.456
Φ_{KJ}	mHz	1.308	1.340
ϕ_J	μHz	24.139	24.830
ϕ_{jk}	μHz	−132.171	−135.342
ϕ_k	mHz	7.352	7.540

values are determined to be about 5.2 (0.53%) and 0.8 cm^{-1} (0.21%) lower than the F12-TZ-cCR data found in Table 5, respectively. This agreement is relatively good, especially for ν_5 which suggests the accuracy of both the experiment and computations. Matrix studies performed by Presilla-Márquez et al. (Presilla-Márquez et al., 1995) considered ν_1 and ν_3 as potential candidates for accurately observed vibrational frequencies of t-Si$_2$C$_2$, and the current work shows values for these modes differing by only 0.4 cm^{-1} (0.03%) for ν_1 at 1537.6 cm^{-1} and 4.9 cm^{-1} (0.78%) for ν_3 at 636.9 cm^{-1} for the F12-TZ-cCR computations found in Table 5. This may be promising for the vibrational observation of ν_3 for t-Si$_2$C$_2$ in the ISM as the intensity is determined to be 63 km mol^{-1}. The lowest energy isomer of cyclic Si$_2$C$_2$ is found to have an anharmonic vibrational intensity of 247 km mol^{-1} for ν_2 at 988.1 cm^{-1}, which is over three times more intense than that of the aforementioned antisymmetric stretch of water. Also, t-Si$_2$C$_2$ is found to have a strong dipole moment of 2.90 D given in Table 6, which suggests the molecule may be rotationally observable if present in high concentrations. This may be likely given the prevalence of SiC dust on chondrite meteorites and in the observed ISM.

The d-Si$_2$C$_2$ isomer with the transannular Si-Si bond displays a strong pseudo-Jahn Teller type-2 distortion effect in the potential energy surface of the molecule (Mintz and Crawford, 2010; Bersuker, 2021). Such behavior causes overlap in the surfaces between this isomer and r-Si$_2$C$_2$. This negates the computation for all of the fundamental vibrational frequencies, but the five that can be determined are reported in Table 5. The one that is missing involves the out-of-plane bend. The coordinates for this motion cause the orbital occupations to collapse to that of the r-Si$_2$C$_2$ isomer where the C_s symmetry is too low to distinguish the wavefunctions in the reference. Even so, the fundamentals reported herein should serve as estimates for any subsequent analysis. Intensities for d-Si$_2$C$_2$ are not computed due to the complexity of the type 2 pseudo-Jahn Teller distortion.

The current work presents the only spectroscopic constants computed at a high level of theory for cyclic Si$_3$C isomers. The r-Si$_3$C species is found to be the lowest energy isomer residing 49.6 kcal mol^{-1} below d-Si$_3$C. Anharmonic vibrational modes of r-Si$_3$C, found in Table 7, computed at the F12-TZ-cCR level compare well with previous experimental matrix studies performed by Presilla-Márquez and Graham (1992) differing by 5.8 cm^{-1} (1.62%) for ν_4 and 5.4 cm^{-1} (1.06%) for ν_3. Similarly, ν_2 shows a maximum difference of 3.2 cm^{-1} (0.49%). Table 8 displays the rotational constants for both isomers. The d-Si$_3$C species may be rotationally observable as the dipole moment for this molecule is determined to be 2.64 D. The d-Si$_3$C isomer has no observable vibrational modes, meaning no modes above JWST's high resolution cutoff of 350 cm^{-1} have an intensity near the anti-symmetric stretch of water, or 70 km mol^{-1}. However, ν_1 of r-Si$_3$C has a higher intensity at 80 km mol^{-1}. This may lead to

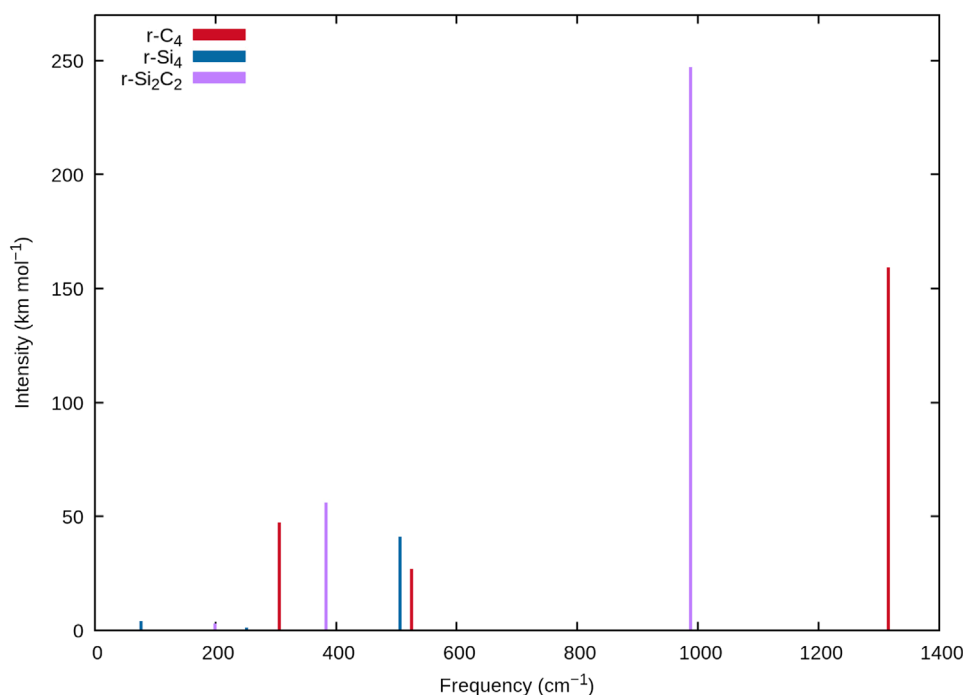**FIGURE 2**
Stick spectra of r-C_4, r-Si_4, and r-Si_2C_2 at the F12-TZ-cCR level of theory showing the decreasing frequencies with Si concentration.

the vibrational observation of this species in the ISM if found in sufficient quantities relative to adjacent molecular species.

Similarly to the previous isomers, this work provides the first high level theoretical spectral data for neutral r-Si_4. Computed spectral data for r-Si_4 are presented in **Tables 9** and **10**. The anharmonic frequency ν_1 may be observable experimentally, as it is shown to have a reasonable intensity of 41 km mol^{-1}.

As silicon composition increases with each TASCC, the current data sheds some light on the effects of silicon doping on the spectral frequencies of tetra-atomic carbon clusters. This is possible due to a similar connectivity between r-C_4, r-Si_2C_2 with a transannular C-C bond, and r-Si_4. **Tables 1**, **5**, and **9** and **Figure 2** demonstrate that the addition of silicon to carbon clusters causes a redshift in each of the vibrational frequencies, agreeing with the work done on larger silicon clusters by Savoca et al. (2013). This can be seen with ν_1 for each species with r-C_4 coming at 1315.1 cm^{-1}, C-C r-Si_2C_2 falling to 1069.7 cm^{-1}, and r-Si_4 coming down to 505.9 cm^{-1}. While such a relationship is expected for heavier atoms, quantification of this relationship may aid in accurately identifying the silicon composition in stellar atmospheres of large carbonaceous stars, or subsequent novae and nebulae. Identifying the molecular framework and elemental ratios in these environments may lead to a more holistic understanding of their processes of formation, i.e. novae processes and the formation of the first interstellar dust grains. With SiC dust making up a large portion of the available cosmic

dust for research on chondrite meteorites, characterization of carbon to silicon ratios in various astronomical environments may lead to a better understanding of the ISM and the processes that lead to its formation but only if data such as those provided herein can be utilized to detect more SiC molecules and clusters.

Conclusion

The most promising anharmonic fundamental frequency for astronomical vibrational detection for these silicon carbide clusters is the ν_2 frequency at 988.1 cm^{-1} (10.1 μm) of r-Si_2C_2 with a transannular C-C bond displaying a very large intensity of 247 km mol^{-1}. This frequency may be a distinct feature in the unidentified IR spectrum and would be a likely candidate for observation if found in sufficient concentrations. Other notable IR features for possible observation include ν_1 of r-C_4 (1315.1 cm^{-1}; 7.6 μm) with an intensity of 159 km mol^{-1}, ν_1 of d-SiC_3 (1339.4 cm^{-1}; 7.5 μm) with an intensity of 128 km mol^{-1}, ν_1 of r-Si_3C (1100.3 cm^{-1}; 9.1 μm) with an intensity of 80 km mol^{-1}, and ν_1 of r-SiC_3 (1525.5 cm^{-1}; 6.6 μm) with an intensity of 77 km mol^{-1}. Each of these anharmonic frequencies are good candidates for observation with the recently operational MIRI instrument aboard the *JWST* between 9.09 μm and 6.56 μm. Finally, rotational observation may be possible for t-Si_2C_2,

d-Si$_3$C, and r-SiC$_3$ due to dipole moments of 2.90, 2.63, and 2.07 D, respectively. Because of this, the prevalence of SiC dust in the ISM, and the known observation of the related d-SiC$_3$, these molecules are strong candidates for radioastronomical observation.

Data availability statement

The original contributions presented in the study are included in the article and **Supplementary Material**, further inquiries can be directed to the corresponding author.

Author contributions

CS performed the computational work with guidance from CP and BW. RF conceived of the idea, managed the project, and secured the funding. All authors were involved in analyzing the results as well as writing and editing the manuscript.

Funding

Acknowledgments

Conflict of interest

The authors declare that the research was conducted in the absence of any commercial or financial relationships that could be construed as a potential conflict of interest.

Publisher's note

All claims expressed in this article are solely those of the authors and do not necessarily represent those of their affiliated organizations, or those of the publisher, the editors and the reviewers. Any product that may be evaluated in this article, or claim that may be made by its manufacturer, is not guaranteed or endorsed by the publisher.

Supplementary material

The Supplementary Material for this article can be found online at: https://www.frontiersin.org/articles/10.3389/fspas.2022.1074879/full#supplementary-material

References

Adler, T. B., Knizia, G., and Werner, H.-J. (2007). A simple and efficient CCSD(T)-F12 approximation. *J. Chem. Phys.* 127, 221106. doi:10.1063/1.2817618

Agbaglo, D., and Fortenberry, R. C. (2019a). The performance of explicitly correlated methods for the computation of anharmonic vibrational frequencies. *Int. J. Quantum Chem.* 119, e25899. doi:10.1002/qua.25899

Agbaglo, D., and Fortenberry, R. C. (2019b). The performance of explicitly correlated wavefunctions [CCSD(T)-F12b] in the computation of anharmonic vibrational frequencies. *Chem. Phys. Lett.* 734, 136720. doi:10.1016/j.cplett.2019.136720

Agbaglo, D., Lee, T. J., Thackston, R., and Fortenberry, R. C. (2019). A small molecule with PAH vibrational properties and a detectable rotational spectrum: c-(C)C$_3$H$_2$, cyclopropenylidenyl carbene. *Astrophys. J.* 871, 236. doi:10.3847/1538-4357/aaf85a

Alberts, I., Grev, R., and Schaefer, H.III (1990). Geometrical structures and vibrational frequencies of the energetically low-lying isomers of SiC$_3$. *J. Chem. Phys.* 93, 5046–5052. doi:10.1063/1.458642

Algranati, M., Feldman, H., Kella, D., Malkin, E., Miklazky, E., Naaman, R., et al. (1989). The structure of C$_4$ as studied by the Coulomb explosion method. *J. Chem. Phys.* 90, 4617–4618. doi:10.1063/1.456597

Allen, W. (2005). *INTDER 2005 is a general program written by W. D. Allen and coworkers, which performs vibrational analysis and higher-order non-linear transformations.* Athens: University of Georgia.

Apponi, A., McCarthy, M., Gottlieb, C. A., and Thaddeus, P. (1999a). Astronomical detection of rhomboidal SiC$_3$. *Astrophys. J.* 516, L103–L106. doi:10.1086/311998

Apponi, A., McCarthy, M., Gottlieb, C. A., and Thaddeus, P. (1999b). The rotational spectrum of rhomboidal SiC$_3$. *J. Chem. Phys.* 111, 3911–3918. doi:10.1063/1.479694

Babin, M., DeWitt, M., Weichman, J., DeVine, M., and Neumark, D. (2021). High-resolution anion photoelectron spectroscopy of cryogenically cooled 4-atom silicon carbides. *Mol. Phys.* 119, e1817596. doi:10.1080/00268976.2020.1817596

Bassett, M. K., and Fortenberry, R. C. (2018). Magnesium in the formaldehyde: The theoretical rovibrational analysis of ˜X3B1 MgCH$_2$. *J. Mol. Spectrosc.* 344, 61–64. doi:10.1016/j.jms.2017.10.012

Bernatowicz, T., Fraundorf, G., Ming, T., Anders, E., Wopenka, B., Zinner, E., et al. (1987). Evidence for interstellar SiC in the Murray carbonaceous meteorite. *Nature* 330, 728–730. doi:10.1038/330728a0

Bersuker, I. (2021). Jahn-Teller and pseudo-Jahn-Teller effects: From particular features to general tools in exploring molecular and solid state properties. *Chem. Rev.* 121, 1463–1512. doi:10.1021/acs.chemrev.0c00718

Bizzocchi, L., Lattanzi, V., Laas, J., Spezzano, S., Giuliano, B. M., Prudenzano, D., et al. (2017). Accurate sub-millimetre rest frequencies for HOCO$^+$ and DOCO$^+$ ions. *Astron. Astrophys.* 602, A34. doi:10.1051/0004-6361/201730638

Blanksby, S., Schröder, D., Dua, S., Bowie, J., and Schwarz, H. (2000). Conversion of linear to rhombic C$_4$ in the gas phase: A joint experimental and theoretical study. *J. Am. Chem. Soc.* 122, 7105–7113. doi:10.1021/ja000951c

Cernicharo, J., Gottlieb, C., Guelin, M., Thaddeus, P., and Vrtilek, J. M. (1989). Astonomical and laboratory detection of the SiC radical. *Astrophys. J.* 341, L25–L28. doi:10.1086/185449

Cernicharo, J., McCarthy, M. C., Gottlieb, C. A., Agúndez, M., Prieto, L. V., Baraban, J. H., et al. (2015). Discovery of SiCSi in IRC+10216: A missing link between gas and dust carriers of Si-C bonds. *Astrophys. J.* 806, L3. doi:10.1088/2041-8205/806/1/l3

Douglas, M., and Kroll, N. (1974). Quantum electrodynamical corrections to the fine structure of helium. *Ann. Phys. (N. Y).* 82, 89–155. doi:10.1016/0003-4916(74)90333-9

Fortenberry, R. C., Huang, X., Crawford, T. D., and Lee, T. J. (2013). High-accuracy quartic force field calculations for the spectroscopic constants and vibrational frequencies of $1^1A'$ l-C_3H^-: A possible link to lines observed in the horsehead nebula PDR. *Astrophys. J.* 772, 39. doi:10.1088/0004-637x/772/1/39

Fortenberry, R. C., Huang, X., Crawford, T. D., and Lee, T. J. (2014a). Quartic force field rovibrational analysis of protonated acetylene, $C_2H_3^+$, and its isotopologues. *J. Phys. Chem. A* 118, 7034–7043. doi:10.1021/jp506441g

Fortenberry, R. C., Huang, X., Francisco, J. S., Crawford, T. D., and Lee, T. J. (2012). Quartic force field predictions of the fundamental vibrational frequencies and spectroscopic constants of the cations $HOCO^+$ and $DOCO^+$. *J. Chem. Phys.* 136, 234309. doi:10.1063/1.4729309

Fortenberry, R. C., Huang, X., Francisco, J. S., Crawford, T. D., and Lee, T. J. (2011). The *trans*-HOCO radical: Fundamental vibrational frequencies, quartic force fields, and spectroscopic constants. *J. Chem. Phys.* 135, 134301. doi:10.1063/1.3643336

Fortenberry, R. C., Huang, X., Schwenke, D. W., and Lee, T. J. (2014b). Limited rotational and rovibrational line lists computed with highly accurate quartic force fields and *ab initio* dipole surfaces. *Spectrochimica Acta Part A Mol. Biomol. Spectrosc.* 119, 76–83. doi:10.1016/j.saa.2013.03.092

Fortenberry, R. C., and Lee, T. J. (2019). Computational vibrational spectroscopy for the detection of molecules in space. *Ann. Rep. Comput. Chem.* 15, 173–202.

Fortenberry, R. C., Lee, T. J., and Müller, H. S. P. (2015). Excited vibrational level rotational constants for SiC_2: A sensitive molecular diagnostic for astrophysical conditions. *Mol. Astrophys.* 1, 13–19. doi:10.1016/j.molap.2015.07.001

Fortenberry, R. C., Novak, C. M., Layfield, J. P., Matito, E., and Lee, T. J. (2018a). Overcoming the failure of correlation for out-of-plane motions in a simple aromatic: Rovibrational quantum chemical analysis of c-C_3H_2. *J. Chem. Theory Comput.* 14, 2155–2164. doi:10.1021/acs.jctc.8b00164

Fortenberry, R. C. (2019). The $ArNH_2^+$ noble gas molecule: Stability, vibrational frequencies, and spectroscopic constants. *J. Mol. Spectrosc.* 357, 4–8. doi:10.1016/j.jms.2019.02.001

Fortenberry, R. C., Trabelsi, T., and Francisco, J. S. (2020). Anharmonic frequencies and spectroscopic constants of OAlOH and AlOH: Strong bonding but unhindered motion. *J. Phys. Chem. A* 124, 8834–8841. doi:10.1021/acs.jpca.0c07945

Fortenberry, R. C., Trabelsi, T., and Francisco, J. S. (2018b). Hydrogen sulfide as a scavenger of sulfur atomic cation. *J. Phys. Chem. A* 122, 4983–4987. doi:10.1021/acs.jpca.8b02923

Fortenberry, R. C., Trabelsi, T., Westbrook, B. R., Del Rio, W. A., and Francisco, J. S. (2019). Molecular oxygen generation from the reaction of water cations with oxygen atoms. *J. Chem. Phys.* 150, 201103. doi:10.1063/1.5102073

Frisch, M. J., Trucks, G. W., Schlegel, H. B., Scuseria, G. E., Robb, M. A., Cheeseman, J. R., et al. (2016). *Gaussian 16 revision C.01*. Wallingford CT: Gaussian Inc.

Gardner, M. B., Westbrook, B. R., Fortenberry, R. C., and Lee, T. J. (2021). Highly-accurate quartic force fields for the prediction of anharmonic rotational constants and fundamental vibrational frequencies. *Spectrochimica Acta Part A Mol. Biomol. Spectrosc.* 248, 119184. doi:10.1016/j.saa.2020.119184

Gaw, J. F., Willets, A., Green, W. H., and Handy, N. C. (1991). "Spectro: A program for the derivation of spectrscopic constants from provided quartic force fields and cubic dipole fields," in *Advances in molecular vibrations and collision dynamics*. Editors J. M. Bowman, and M. A. Ratner (Greenwich, Connecticut: JAI Press, Inc.), 170.

Hill, J. G., and Peterson, K. A. (2010). Correlation consistent basis sets for explicitly correlated wavefunctions: Valence and core-valence basis sets for Li, Be, Na, and Mg. *Phys. Chem. Chem. Phys.* 12, 10460–10468. doi:10.1039/c0cp00020e

Huang, X., Fortenberry, R. C., and Lee, T. J. (2013). Protonated nitrous oxide, $NNOH^+$: Fundamental vibrational frequencies and spectroscopic constants from quartic force fields. *J. Chem. Phys.* 139, 084313. doi:10.1063/1.4819069

Huang, X., and Lee, T. J. (2008). A procedure for computing accurate *ab initio* quartic force fields: Application to HO_2^+ and H_2O. *J. Chem. Phys.* 129, 044312. doi:10.1063/1.2957488

Huang, X., and Lee, T. J. (2009). Accurate *ab initio* quartic force fields for NH_2^- and CCH^- and rovibrational spectroscopic constants for their isotopologs. *J. Chem. Phys.* 131, 104301. doi:10.1063/1.3212560

Huang, X., Taylor, P. R., and Lee, T. J. (2011). Highly accurate quartic force field, vibrational frequencies, and spectroscopic constants for cyclic and linear $C_3H_3^+$. *J. Phys. Chem. A* 115, 5005–5016. doi:10.1021/jp2019704

Huang, X., Valeev, E. F., and Lee, T. J. (2010). Comparison of one-particle basis set extrapolation to explicitly correlated methods for the calculation of accurate quartic force fields, vibrational frequencies, and spectroscopic constants: Application to H_2O, N_2H^+, NO_2^+, and C_2H_2. *J. Chem. Phys.* 133, 244108. doi:10.1063/1.3506341

Inostroza, N., Hochlaf, M., Senent, M., and Letelier, J. (2008). *Ab initio* characterization of linear C_3Si Isomers. *Astron. Astrophys.* 486, 1047–1052. doi:10.1051/0004-6361:200809556

Kitchens, M. J. R., and Fortenberry, R. C. (2016). The rovibrational nature of closed-shell third-row triatomics: HOX and HXO, X = Si^+, P, S^+, and Cl. *Chem. Phys.* 472, 119–127. doi:10.1016/j.chemphys.2016.03.018

Knizia, G., Adler, T. B., and Werner, H.-J. (2009). Simplified CCSD(T)-F12 methods: Theory and benchmarks. *J. Chem. Phys.* 130, 054104. doi:10.1063/1.3054300

Lammertsma, K., and Güner, O. F. (1988). Structures and energies of disilicon dicarbide, C2Si2. C_2Si_2. *J. Am. Chem. Soc.* 110, 5239–5245. doi:10.1021/ja00224a001

Lavendy, H., Robbe, J., Flament, J., and Pascoli, G. (1997). Density functional study of small silicon carbide cluster cations C_4^+, C_3Si^+, $C_2Si_2^+$, CSi_3^+, and Si_4^+. *J. Chim. Phys.* 94, 1779–1793. doi:10.1051/jcp/1997941779

Linguerri, R., Rosmus, P., and Carter, S. (2006). Anharmonic vibrational levels of the two cyclic isomers of SiC_3. *J. Chem. Phys.* 125, 034305. doi:10.1063/1.2209693

Martin, J. M. L., and Taylor, P. R. (1997). Accurate *ab initio* quartic force field for *trans*-HNNH and treatment of resonance polyads. *Spectrochimica Acta Part A Mol. Biomol. Spectrosc.* 53, 1039–1050. doi:10.1016/s1386-1425(96)01869-0

Martin, J. M. L., and Taylor, P. R. (1996). Structure and vibrations of small carbon clusters from coupled-cluster calculations. *J. Phys. Chem.* 100, 6047–6056. doi:10.1021/jp952471r

Martin, J., Schwenke, D., Lee, T., and Taylor, P. R. (1996). Is there evidence for detection of cyclic C_4 in IR spectra? An accurate *ab initio* computed quartic force field. *J. Chem. Phys.* 104, 4657–4663. doi:10.1063/1.471212

Matthews, L., Hayes, R., Michael, S., Freed, T., and Hyde, W. (2007). Formation of cosmic dust bunnies. *IEEE Trans. Plasma Sci. IEEE Nucl. Plasma Sci. Soc.* 35, 260–265. doi:10.1109/tps.2007.892718

McCarthy, M., Apponi, A., and Thaddeus, P. (1999). A second rhomboidal isomer of SiC_3. *J. Chem. Phys.* 111, 7175–7178. doi:10.1063/1.480044

McCarthy, M. C., Gottlieb, C. A., and Cernicharo, J. (2019). Building blocks of dust: A coordinated laboratory and astronomical study of the archtype Agb carbon star IRC+10216. *J. Mol. Spectrosc.* 356, 7–20. doi:10.1016/j.jms.2018.11.018

Mélinon, P., Masenelli, B., Tournus, F., and Perez, A. (2007). Playing with carbon and silicon at the nanoscale. *Nat. Mat.* 6, 479–490. doi:10.1038/nmat1914

Mills, I. M. (1972). "Vibration-rotation structure in asymmetric- and symmetric-top molecules," in *Molecular spectroscopy - modern research*. Editors K. N. Rao, and C. W. Mathews (New York: Academic Press), 115–140.

Mintz, B., and Crawford, T. D. (2010). Symmetry breaking in the cyclic C_3C_2H radical. *Phys. Chem. Chem. Phys.* 12, 15459–15467. doi:10.1039/c0cp00864h

Nittler, L., and Alexander, C. (2003). Automated isotopic measurements of micron-sized dust: Application to meteoritic presolar silicon carbide. *Geochimica Cosmochimica Acta* 67, 4961–4980. doi:10.1016/s0016-7037(03)00485-x

Papousek, D., and Aliev, M. R. (1982). *Molecular vibration-rotation spectra*. Amsterdam: Elsevier.

Peterson, K. A., Adler, T. B., and Werner, H.-J. (2008). Systematically convergent basis sets for explicitly correlated wavefunctions: The atoms H, He, B-Ne, and Al-Ar. *J. Chem. Phys.* 128, 084102. doi:10.1063/1.2831537

Presilla-Márquez, J., Gay, S., Rittby, C., and Graham, W. R. M. (1995). Vibrational spectra of tetra-atomic silicon– carbon clusters. II. Si_2C_2 in Ar at 10 K. *J. Chem. Phys.* 102, 6354–6361. doi:10.1063/1.469352

Presilla-Márquez, J., and Graham, W. (1992). Vibrational spectra of tetra-atomic silicon– carbon clusters. I. rhomboidal Si_3C in Ar at 10 K. *J. Chem. Phys.* 96, 6509–6514. doi:10.1063/1.462588

Prieto, L. V., Cernicharo, J., Quintana-Lacaci, G., Agúndez, M., Castro-Carrizo, A., Fonfría, J. P., et al. (2015). Si-Bearing molecules toward IRC+10216: ALMA unveils the molecular envelope of CWLeo. *Astrophys. J.* 805, L13. doi:10.1088/2041-8205/805/2/l13

Raghavachari, K., Trucks, G. W., Pople, J. A., and Head-Gordon, M. (1989). A fifth-order perturbation comparison of electron correlation theories. *Chem. Phys. Lett.* 157, 479–483. doi:10.1016/s0009-2614(89)87395-6

Rittby, C. M. L. (1992). An *ab initio* study of the structure and infrared spectrum of Si_3C. *J. Chem. Phys.* 96, 6768–6772. doi:10.1063/1.462564

Savoca, M., Lagutschenkov, A., Langer, J., Harding, D., Fielicke, A., and Dopfer, O. (2013). Vibrational spectra and structures of neutral Si_mC_n clusters (m + n = 6): Sequential doping of silicon clusters with carbon atoms. *J. Phys. Chem. A* 117, 1158–1163. doi:10.1021/jp305107f

Savoca, M., Langer, J., Harding, D., Dopfer, O., and Fielicke, A. (2012). Incipient chemical bond formation of Xe to a cationic silicon cluster: Vibrational spectroscopy and structure of the Si_4Xe+ complex. *Chem. Phys. Lett.* 557, 49–52. doi:10.1016/j.cplett.2012.12.020

Stanton, J., Dudek, J., Theulé, P., Gupta, H., McCarthy, M. C., and Thaddeus, P. (2005). Laser spectroscopy of Si_3C. *J. Chem. Phys.* 122, 124314. doi:10.1063/1.1869981

Thaddeus, P., Cummins, S. E., and Linke, R. A. (1984). Identification of the SiCC radical toward IRC +10216: The first molecular ring in an astronomical source. *Astrophys. J.* 283, L45–L48. doi:10.1086/184330

Truong, N., Savoca, M., Harding, D., Fielicke, A., and Dopfer, O. (2015). Vibrational spectra and structures of Si_nC clusters (n = 3–8). *Phys. Chem. Chem. Phys.* 17, 18961–18970. doi:10.1039/c5cp02588e

Valiev, R. R., Nasibullin, R. T., Cherepanov, V. N., Baryshnikov, G. V., Sundholm, D., Ågren, H., et al. (2020). First-principles calculations of anharmonic and deuteration effects on the photophysical properties of polyacenes and porphyrinoids. *Phys. Chem. Chem. Phys.* 22, 22314–22323. doi:10.1039/d0cp03231j

Varandas, A., and Rocha, C. (2018). $C_n (n = 2 − 4)$: Current status. *Phil. Trans. R. Soc. A* 376, 20170145. doi:10.1098/rsta.2017.0145

Wang, X., Bowman, J. M., and Lee, T. J. (2013). Anharmonic rovibrational calculations of singlet cyclic C_4 using a new *ab initio* potential and a quartic force field. *J. Chem. Phys.* 139, 224302. doi:10.1063/1.4837177

Wang, Z. D., and Whithey, P. A. (2018). Comprehensive survey of the structures of C_4, $C_4^−$ and C_4^+ Clusters. *ChemistrySelect* 3, 13355–13364. doi:10.1002/slct.201801831

Watrous, A. G., Westbrook, B. R., and Fortenberry, R. C. (2021). F12-TZ-cCR: A methodology for faster and still highly-accurate quartic force fields. *J. Phys. Chem. A* 125, 10532–10540. doi:10.1021/acs.jpca.1c08355

Watson, J. K. G. (1977). "Aspects of quartic and sextic centrifugal effects on rotational energy levels," in *Vibrational spectra and structure*. Editor J. R. During (Amsterdam: Elsevier), 1–89.

Werner, H.-J., Knowles, P. J., Manby, F. R., Black, J. A., Doll, K., Heßelmann, A., et al. (2020). Molpro, version 2020.1, a package of *ab initio* programs. *WIREs Comput. Mol. Sci.* 2012, 242. doi:10.1002/wcms.82

Westbrook, B. R., and Fortenberry, R. C. (2020). Anharmonic frequencies of $(MO)_2$ & related hydrides for M = Mg, Al, Si, P, S, Ca, & Ti and heuristics for predicting anharmonic corrections of inorganic oxides. *J. Phys. Chem. A* 124, 3191–3204. doi:10.1021/acs.jpca.0c01609

Yadav, P., Yadav, R., Agrawal, S., and Agrawal, B. (2006). Theoretical study of the physical properties of binary Si_mC_n (m+n>5) clusters: An *ab initio* study. *Phys. E Low-dimensional Syst. Nanostructures* 33, 249–262. doi:10.1016/j.physe.2006.03.132

Zhao, D., Doney, K. D., and Linnartz, H. (2014). Laboratory gas-phase detection of the cyclopropenyl cation (c-$C_3H_3^+$). *Astrophys. J.* 791, L28. doi:10.1088/2041-8205/791/2/l28